Smart Structures and Systems, *Vol. 28, No. 5 (2021) 605-615*
https://doi.org/10.12989/sss.2021.28.5.605

Controller and sensor placement for a 3D irregular building based on Hankel norm

Yumei Wang*[1a] and Shirley J. Dyke [2b]

[1] *Earthquake Engineering Research and Test Center, Guangzhou University, Guangzhou, China*
[2] *Department of Mechanical Engineering and Civil Engineering, Purdue University, 550 Stadium Mall Drive, West Lafayette, IN 47907-2051, USA*

(*Received January 9, 2021, Revised June 11, 2021, Accepted June 12, 2021*)

Abstract. Placing controllers and sensors properly is important in structural health monitoring and control. Many optimization methods require much computation efforts. This paper used Hankel norms to develop the placement rules, because they involve the input and output gains and thus could be shaped by the locations. In modal form, their computations are relatively simple. The location and mode influences on norms were arranged in rows and columns, respectively, to form a matrix, and was normalized by the column (mode) root mean square. The optimization goal is to choose locations with higher index values and lower correlations to ensure higher controllability and observability, and with less effort to be compensated for by gains. Hankel norm is compatible with the LQR control objectives in that they are both 2-norm, so the methodology is appropriate to be applied to the base isolation benchmark building for structural control, which is an eight-story irregular building with ninety-two candidate locations for controllers and thirty-six locations for sensors. Following the method, ten controller locations and eighteen sensor locations were determined. Earthquake time history analysis using LQG technique validated the effectiveness of thus determined subset of locations by comparing with other subset of locations.

Keywords: controllability and observability; controller and sensor placement; Hankel singular norm; non-collocated system; placement index

1. Introduction

Controlling and measuring at proper locations is very important in structural health monitoring, structural control and robotics. Placement is in the first place a problem of optimization on control (or measuring) objectives and evaluation criteria. So, most procedures for solving the problems involve optimization techniques (such as minimizing objective functions, Genetic Algorithm (GA), etc.) and Modal Identification (MI) techniques. Placement is also a problem of simplification, because it is specially required in complex and large-scale structures, and so model reduction techniques and sub-structure procedures are popular as well. Other objective functions and criteria for the placement determination include: the Fisher Information Matrix (FIM), Modal Assurance Criterion (MAC), and Mean Square Error (MSE) of mode shapes, Information Entropy (IE) Method, etc.

For example, Soman *et al*. (2014) presented a multi-objective optimization strategy for health monitoring of long span bridges through MI and accurate mode shape expansion. He *et al*. (2015) formulated an optimization procedure with the objective of minimizing sensors and cost through reconstructing structural responses as feedbacks. Casciati and Faravelli (2014) took sensor readings as the inputs of a reduced-order numerical model, and located the sensors with the goal of minimizing the deviations from the responses of the true (full) model. Tong *et al*. (2014) proposed an improved simulated annealing algorithm for the sensor placement problem, with FIM, and MSE as criteria to validate the method. Lu *et al*. (2015) proposed a method for the MI of truss structures based on structural sub-section and model reduction techniques, with the optimal objective function solved by GA. Leyder *et al*. (2018) investigated three methods: the effective independence method, the Modal Kinetic Energy method and the IE Method to resolve the problem of close positioning of sensors in terms of three metrics: the IE index, MAC and a relative dispersion index. Reichert *et al*. (2020) proposed a combined approach of FIM and MSE in a two-step procedure, and applied it on a finite element model and validated the results by laboratory experiments. Kaur *et al*. (2019) proposed a weighted centroid DV-Hop algorithm that considers the influence of anchor numbers, communication radius, and nearest anchor to determine location of unknown node.

For cases where controller and sensor are not collocated, internal and cross couplings of the inputs, measurements, and regulated outputs have to be accounted for, because these effects all impact on the structural dynamic properties. Yang (1997) discussed the problem and developed stability criteria, design guidelines and control law selection for the non-collocated system. Majumder and Khaparde (2016)

*Corresponding author, Associate Professor,
E-mail: ymwang@gzhu.edu.cn
[a] Professor, E-mail: sdyke@purdue.edu

ISSN: 1738-1584 (Print), 1738-1991 (Online)

described an optimal scheduling of multiple non-collocated wind turbine generators and battery storage devices participating in forward day-ahead distribution electricity market through minimizing the objective function which is dependent upon the location of wind power producers in the network.

However, these algorithms usually require high computational efforts. Studies showed that, the internal and cross couplings all impact on the structural norms due to the feedback loop. So, norm-based properties e.g., the infinite norms (Silva *et al*. 2004), were also suitable for placement problems. Among which, methods based on the controllability and observability Grammians have many applications in control problems. These properties can be shaped by changing the configuration of the actuators and sensors. This is done by establishing explicit relationships between controllability and observability with system matrices (Moore 1981). Choi *et al*. (2000) introduced the magnitude of the measures and the norms of eigenvectors in the balanced coordinate system. Kang and Shin (2016) determined the accelerometer locations for bridges using the frequency-domain Hankel matrix, which is related to the eigenvalues of the cross-Grammians. Le *et al*. (2016) determined the optimal location of the thyristor-controlled series compensator, in which feasible locations were searched using the combination of the controllability Grammian with the balanced realization reduction technique. Gawronski (1998) used the Hankel norm in modal coordinate system to develop the placement rule and LQG control strategies, because Hankel norms agree with the control objective of the LQR method. Bigoni *et al*. (2020) proposed to use the variational approximation of sparse Gaussian processes to systematically place a fixed number of sensors over a structure of interest, with identifying the optimal locations that maximize the observability of the discriminant features as the goal. The healthy parametric variations of the structure are included by clustering the inducing inputs, i.e., the outcome of variational inference. Bopardikar (2021) provide a probabilistic treatment to the sensor placement in a set of candidate locations such that the observability Grammian of the resulting placement is sufficiently non-singular.

This study would apply the Hankel norm-based method to the smart base isolation benchmark building, which is suitable for this system with internal and cross couplings of: the seismic input with the structural responses; the lateral degrees of freedom (DOFs) with torsion DOFs due to irregularities; the controller at the base with the feedback from upper-level sensors; and the non-collocation of controllers with sensors.

2. Influence of measurements on the regulated outputs in a feedback system

This section discusses theoretically the impacts of non-collocated measurements and regulated outputs on the control effects and structural responses.

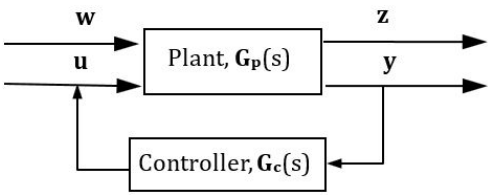

Fig. 1 General diagram of a feedback control system

Let lower case letters represent the time-domain variables, and capital letters represent their Laplace transfer. A structure's inputs are composed of disturbance $\boldsymbol{w}$ and control input $\boldsymbol{u}$, while the outputs include regulated outputs $\boldsymbol{z}$ and measurement outputs$\boldsymbol{y}$. For non-collocated systems, $\boldsymbol{y} \neq z$. $\boldsymbol{G}_p(s)$ and $\boldsymbol{G}_c(s)$ are the open-loop transfer functions of the plant and the controller, respectively. The block diagram of a general feedback control system is shown Fig. 1.

The equations of motion of the closed-loop system in Fig. 1 is Eqs. (1)-(2)

$$\dot{\boldsymbol{x}}(t) = \boldsymbol{A}\boldsymbol{x}(t) + [\boldsymbol{B} \quad \boldsymbol{E}]\begin{bmatrix}\boldsymbol{u}(t)\\ \boldsymbol{w}(t)\end{bmatrix} \tag{1}$$

$$\begin{bmatrix}\boldsymbol{z}(t)\\ \boldsymbol{y}(t)\end{bmatrix} = \begin{bmatrix}\boldsymbol{C}_z\\ \boldsymbol{C}_y\end{bmatrix}\boldsymbol{x}(t) + \begin{bmatrix}\boldsymbol{D}_z & \boldsymbol{E}_z\\ \boldsymbol{D}_y & \boldsymbol{E}_y\end{bmatrix}\begin{bmatrix}\boldsymbol{u}(t)\\ \boldsymbol{w}(t)\end{bmatrix} \tag{2}$$

where $\boldsymbol{A}$ is state matrix, $\boldsymbol{B}$ is the influence matrix of control input, $\boldsymbol{C}$ is the output gain matrix, $\boldsymbol{D}$ and $\boldsymbol{E}$ are the influence matrices of disturbance. The information of the controller location is contained in matrix $\boldsymbol{B}$, and the information of sensor locations is reflected in the matrix $\boldsymbol{C}$.

Let $\boldsymbol{G_{wz}}$, $\boldsymbol{G_{wy}}$, $\boldsymbol{G_{uz}}$, $\boldsymbol{G_{uy}}$ be the open-loop transfer functions from $\boldsymbol{w}$ to $\boldsymbol{z}$, $\boldsymbol{w}$ to $\boldsymbol{y}$, $\boldsymbol{u}$ to $\boldsymbol{z}$, and $\boldsymbol{u}$ to $\boldsymbol{y}$, respectively, the Laplace transform of Eq. (2) is then written into Eq. (3)

$$\begin{aligned}\begin{bmatrix}\boldsymbol{Z}\\ \boldsymbol{Y}\end{bmatrix} &= \boldsymbol{G}_p(s)\begin{bmatrix}\boldsymbol{U}\\ \boldsymbol{W}\end{bmatrix} = \begin{bmatrix}\boldsymbol{G_{uz}} & \boldsymbol{G_{wz}}\\ \boldsymbol{G_{uy}} & \boldsymbol{G_{wy}}\end{bmatrix}\begin{bmatrix}\boldsymbol{U}\\ \boldsymbol{W}\end{bmatrix}\\ &= \begin{bmatrix}\boldsymbol{G_{uz}U} + \boldsymbol{G_{wz}W}\\ \boldsymbol{G_{uy}U} + \boldsymbol{G_{wy}W}\end{bmatrix}.\end{aligned} \tag{3}$$

If controller force $\boldsymbol{U} = \boldsymbol{G_c Y}$, then substituting $\boldsymbol{Y}$ of the second Eq. (3) into it, it yields Eq. (4), where $\boldsymbol{I}$ represents unit matrix

$$\boldsymbol{U} = (\boldsymbol{I} - \boldsymbol{G_c G_{uy}})^{-1}\boldsymbol{G_c G_{wy} W}. \tag{4}$$

Substituting Eq. (4) into the first Eq. (3) yields the closed-loop transfer function (from $\boldsymbol{w}$ to $\boldsymbol{z}$) $\boldsymbol{G_{wz}}$, of the feedback control system (Eq. (5))

$$\boldsymbol{Z} = \boldsymbol{G_{wz}W} = (\boldsymbol{G_{uz}}\big(\boldsymbol{I} - \boldsymbol{G_c G_{uy}}\big)^{-1}\boldsymbol{G_c G_{wy}} + \boldsymbol{G_{wz}}\big)\boldsymbol{W}. \tag{5}$$

For a constant gain case, i.e., $\boldsymbol{G_c} = \boldsymbol{K}$, the closed-loop transfer function of the plant $\boldsymbol{G_{p-cl}}$ becomes Eq. (6)

$$\boldsymbol{G_{p-cl}} = \boldsymbol{G_{uz}}(\boldsymbol{I} - \boldsymbol{K G_{uy}})^{-1}\boldsymbol{K G_{wy}} + \boldsymbol{G_{wz}}. \tag{6}$$

So, for non-collocated systems, the importance of locations to the closed-loop performance is not only determined by the value of $\boldsymbol{G_{uy}}$. If either $\boldsymbol{G_{wy}}$ or $\boldsymbol{G_{uz}}$ is zero, the actuator could not reach$\boldsymbol{z}$. But for collocated systems, this cross-actions does not exist, because$\boldsymbol{y} = \boldsymbol{z}$, $\boldsymbol{G_{wy}} = \boldsymbol{G_{wz}}$, and $\boldsymbol{G_{uy}} = \boldsymbol{G_{uz}}$. Thus $\boldsymbol{G_{p-cl}}$ becomes Eq. (7)

$$\boldsymbol{G_{p-cl}} = (\boldsymbol{I} - \boldsymbol{K}\boldsymbol{G_{uz}})^{-1}\boldsymbol{G_{wz}} \tag{7}$$

.

The cross-couplings make the placement problem complicated. Fortunately, the approximate multiplicative property in modal coordinates of Eq. (8) holds (Gawronski 1998)

$$\|\boldsymbol{G_{wz,i}}\| \times \|\boldsymbol{G_{uy,i}}\| \cong \|\boldsymbol{G_{wy,i}}\| \times \|\boldsymbol{G_{uz,i}}\| \tag{8}$$

where $\|.\|$ denotes either H_2, H_∞, or Hankel norms, and subscript i denotes the i^{th} mode.

This property indicates that, the transfer function and the norms are internally related. For each mode, the product of the performance loop and the control loop is approximately equal to the product of their cross couplings, which means that, improvement in $\boldsymbol{G_{uy}}$ automatically leads to improvement in $\boldsymbol{G_{wy}}$ and $\boldsymbol{G_{uz}}$. Thus, the actuator and sensor location problems can be performed by manipulating the norm of transfer function of $\boldsymbol{G_{uy}}$ alone in modal coordinate system. This conclusion is important for the placement problem. It means that, the placement strategy based on modal Hankel norms would be appropriate for the placement of non-collocated systems.

3. Study case: the placement problem in the benchmark building for structural control

The ASCE Committee on Structural Control developed a smart base isolation benchmark problem for use by the research community to evaluate their control strategies (2002, 2004), including the control devices, algorithms, and sensors, etc. The benchmark model is an eight-story base isolated building: the floor plan is L-shaped and has setbacks above the fifth floor. The superstructure is supported on a reinforced concrete base slab, where the isolators to be installed. The nominal isolation system consists of ninety-two bearings. Participants may develop their own device models, and place their devices at their desired locations. The available locations at the base level, stories, installation schematic are shown on Fig. 2. The final determined set of locations (red arrows) and a non-optimal set of locations for comparison are also shown on Fig. 2 (green circles).

Narasimhan *et al*. (2002) have developed a 3D model of the entire system. For details about the parameters of the superstructure, the equations, matrices and point coordinates of the 3D model, please refer to the problem definition of the above two papers.

The isolation parameters used in this study, i.e., total bearing stiffness and damping coefficient of the bearings, are: $k_b = 2119.4$ kN/m, $c_b = 241.44$ kN-s/m, resulting in fundamental periods of 2.28 sec (x-), 2.18 sec (y-), and 1.86 sec (r-) and damping ratios of $\xi_1 = 14.7\%$ (x-), $\xi_2 =$

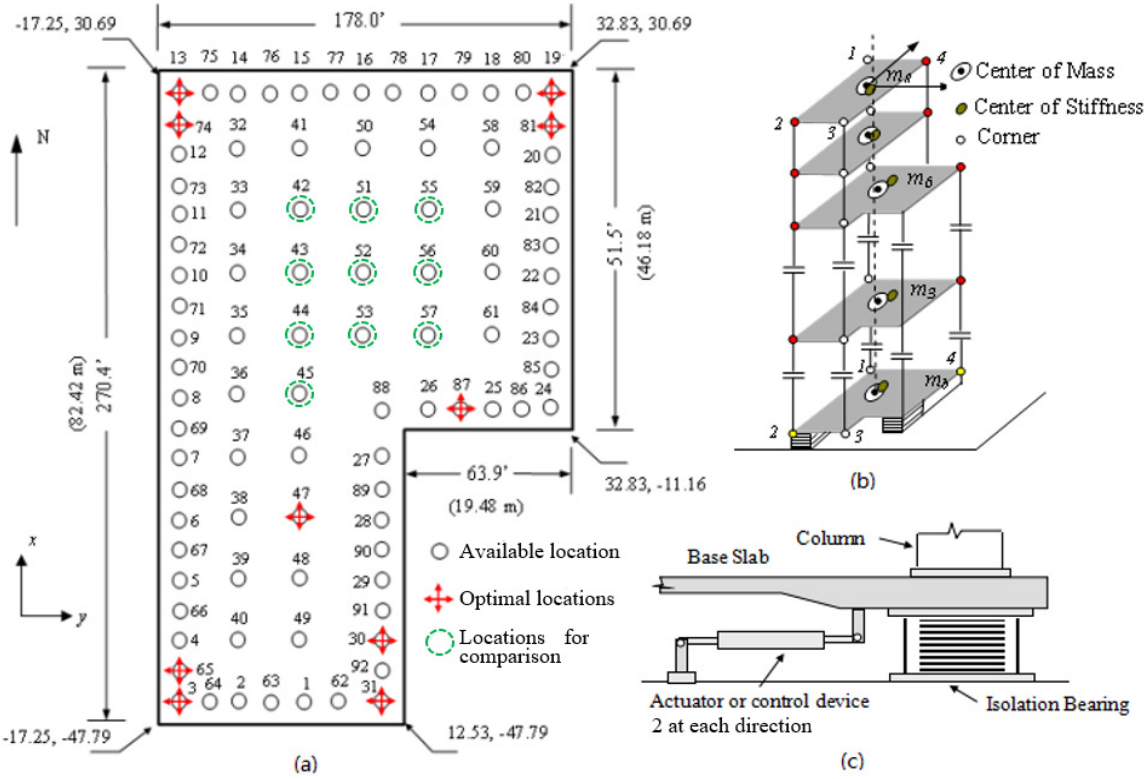

Fig. 2 Device placement of the benchmark building: (a) bearings/controllers at the base level; (b) sensors on the stories; (c) bearing/controller installation

14.9% (y-), and $\xi_3 = 17.9\%$ (r-). These are appropriate for a traditional passive isolation design for near-source protection. The damping ratios are less than 20%, so it is reasonable if additional damping from an MR damper is to be applied on this passive optimal system.

The benchmark problem requires the control devices to be placed at base level and, conveniently, at bearing locations. It is neither possible nor necessary to install the controllers at all 92 available locations; also, accelerometers may be placed at the far-end corners of each floor (including the base), and displacement sensors may be placed at the corners of the base. Each corner has one accelerometer in the *x*- and one in the *y*-direction, which gives eight available accelerometer locations for each floor. Note that 3 sensors would be enough for each floor to capture the responses, because each floor has 3 DOFs. The planar and vertical irregularity increased the difficulty of the problem. So, this placement problem is to determine a reasonable subset of locations for control devices that offer high controllability of the desired modes, and a reasonable subset of sensors that offer high observability in detecting of the desired modes.

4. Placement method

4.1 Hankel norms in modal coordinate system

Both $\boldsymbol{u}$ and $\boldsymbol{w}$ are structural inputs. However, $\boldsymbol{w}$ is the external disturbance. The accompanying gain $\boldsymbol{E}$ is independent of structure, i.e., it is not to be designed. On the contrary, the control gain $\boldsymbol{B}$ can be influenced by the configuration of control devices, and subsequently, structural properties. Making controls more efficient and adaptable to general disturbances through adjustment of structural internal properties is the objective of this study. So, herein it is assumed $\boldsymbol{w} = 0$ in Eq. (1).

Let $\boldsymbol{T}$ be the matrix that transforms the state vector $\boldsymbol{x}$ to a new state vector $\bar{\boldsymbol{x}}$, i.e., $\boldsymbol{x} = \boldsymbol{T}\bar{\boldsymbol{x}}$. Substituting $\boldsymbol{x} = \boldsymbol{T}\bar{\boldsymbol{x}}$ into the state Eq. (1) produces Eq. (9)

$$\dot{\bar{\boldsymbol{x}}} = \boldsymbol{A}_m\bar{\boldsymbol{x}} + \boldsymbol{B}_m\boldsymbol{u}, \quad \text{and} \quad \boldsymbol{y} = \boldsymbol{C}_m\bar{\boldsymbol{x}} + \boldsymbol{D}_m\boldsymbol{u} \tag{9}$$

When $\boldsymbol{T}^{-1}\boldsymbol{A}\boldsymbol{T}$ is diagonal or block diagonal, the state-space representation can be denoted by the modal triple $(\boldsymbol{A}_m, \boldsymbol{B}_m, \boldsymbol{C}_m)$ (matrix $\boldsymbol{D}$ is invariant) and

$$\begin{aligned} \boldsymbol{A}_m &= \boldsymbol{\Lambda} = \boldsymbol{T}^{-1}\boldsymbol{A}\boldsymbol{T}, \quad & \boldsymbol{B}_m &= \boldsymbol{T}^{-1}\boldsymbol{B}, \\ \boldsymbol{C}_m &= \boldsymbol{C}_y\boldsymbol{T}, & \boldsymbol{D}_m &= \boldsymbol{D}_y \end{aligned} \tag{10}$$

The modal form that civil engineers traditionally use is the one with eigenvalues on the diagonal. However, eigenvalues could be complex values. In structural control, the real block-diagonal form is preferred. The real block-diagonal of the i^{th} mode is as in Eq. (11)

$$\begin{aligned} &\boldsymbol{B}_m = {\boldsymbol{T}_{21}}^{-1}\boldsymbol{B}, \qquad \boldsymbol{A}_{mi} = \begin{bmatrix} -\zeta_i\omega_i & \omega_i \\ -\omega_i & -\zeta_i\omega_i \end{bmatrix}, \\ &\boldsymbol{T}_{21,i} = \begin{bmatrix} 1 & 0 \\ -\varsigma_i\omega_i & \omega_i \end{bmatrix} \end{aligned} \tag{11}$$

where $\boldsymbol{T}_{21}$ is the transformation matrix from the traditional eigen-matrix.

Using real block-diagonal form, the controllability grammian $w_{c,i}$, observability grammian $w_{c,o}$, and the Hankel norm of the i^{th} modeγ_i, can be obtained from the approximate analytical equations of

$$w_{c,i} = \frac{\left\|\boldsymbol{B}_{m,i}\right\|_2^2}{4\zeta_i\omega_i}, \qquad w_{c,o} = \frac{\left\|\boldsymbol{C}_{m,i}\right\|_2^2}{4\zeta_i\omega_i}. \tag{12}$$

where, (ω_i, ζ_i) are the polar frequency and damping ratio of the i^{th} mode, respectively, and $\|.\|_2$ denotes the 2-norm. Grammians vary with different coordinate systems. However, the eigenvalues of their product matrix are invariant. Hankel norm $\|\boldsymbol{G}\|_h$ is defined as: $\|\boldsymbol{G}\|_h = \lambda\left(\sqrt{\boldsymbol{W}_o\boldsymbol{W}_c}\right)$ (where λ denotes eigenvalue). It is a measure of the amount of energy stored in and subsequently retrieved from the system (Boyd and Barratt 1991).

In modal coordinates, Hankel norms of the i^{th} mode can be obtained by approximate analytical equations, and the Hankel norm of the system is the largest norm of all modes, which is shown in Eq. (13)

$$\begin{aligned} &\|\boldsymbol{G}_i\|_h = \gamma_i \cong \frac{\|\boldsymbol{B}_{mi}\|_2\|\boldsymbol{C}_{mi}\|_2}{4\xi_i\omega_i}, \\ &\|\boldsymbol{G}\|_h \cong \max_i\|\boldsymbol{G}_i\|_h = \gamma_{max} \end{aligned} \tag{13}$$

It can be seen that, Hankel norm involves both the input and the output gains, and thus can be used in actuator/sensor placement. In addition, by approximate modal Eqs. (12)-(13), the computation of Grammians and Hankel norms are much easier than in nodal coordinates.

In the text, the term "actuator" will be used for generality. It applies to all devices that may change the matrix $\boldsymbol{B}_m$, such as bearings, passive or semi-active dampers, controllers, etc. Similarly, sensors could be accelerometers or other gauges, as long as they influence the matrix $\boldsymbol{C}_m$.

4.2 Placement indices based on Hankel norms

The question then arises as to how the Hankel norm of a structure with single control device or sensor relates to the Hankel norm with *s* actuators or *r* sensors. It turns out that, for each mode, the Hankel norm with a set of actuators or sensors is the root mean square (RMS) sum of the Hankel norm with each single actuator or sensor from this set, i.e.,

$$\gamma_i = \sqrt{\sum_{j=1}^{s}\gamma_{ij}^2}, \qquad \gamma_i = \sqrt{\sum_{k=1}^{r}\gamma_{ik}^2}. \tag{14}$$

Eq. (14) provide a means to normalize the indices using Hankel norms so that the indices are between 0 and 1.

For actuator (sensor) placement, the index σ_{ij} (σ_{ik}) that evaluates the j^{th} actuator (the k^{th} sensor) at the i^{th} mode in terms of Hankel norm is defined with respect to all modes and all devices. These are shown in Eq. (15)

$$\sigma_{ij} = \frac{\|G_{ij}\|_h}{\|\boldsymbol{G}\|_h}, \qquad \sigma_{ik} = \frac{\|G_{ik}\|_h}{\|\boldsymbol{G}\|_h}. \tag{15}$$

It is convenient to arrange the placement indices in the matrix. The resulting actuator and sensor placement index matrix is (Gawronski 1998)

$$\begin{bmatrix} \sigma_{11} & \sigma_{21} & \cdots & \sigma_{i1} & \cdots & \sigma_{n1} \\ \sigma_{21} & \sigma_{22} & \cdots & \sigma_{i2} & \cdots & \sigma_{n2} \\ \cdots & \cdots & \cdots & \cdots & \cdots & \cdots \\ \sigma_{1j} & \sigma_{2j} & \cdots & \sigma_{ij} & \cdots & \sigma_{nj} \\ \cdots & \cdots & \cdots & \cdots & \cdots & \cdots \\ \sigma_{1s} & \sigma_{2s} & \cdots & \sigma_{is} & \cdots & \sigma_{ns} \end{bmatrix} \Longleftarrow j\text{th actuator}$$
$$\Uparrow$$
$$j\text{th mode}$$

The placement index can be studied from two points of views. First, one may examine the importance of a single actuator/sensor over all modes, i.e., rows of the matrices (16), using column Eq. (17)

$$\text{Controller index vector:} \quad \boldsymbol{\sigma}_A = [\boldsymbol{\sigma}_{A1} \quad \boldsymbol{\sigma}_{A2} \quad \cdots \quad \boldsymbol{\sigma}_{As}]^T \tag{17a}$$

$$\text{Sensor index vector:} \quad \boldsymbol{\sigma}_S = [\boldsymbol{\sigma}_{S1} \quad \boldsymbol{\sigma}_{S2} \quad \cdots \quad \boldsymbol{\sigma}_{Sr}]^T \tag{17b}$$

where the k^{th} entry is the placement index of the k^{th} control device/sensor, the subscript A represent actuator and S represent the sensor. In the case of the Hankel norm

$$\boldsymbol{\sigma}_{Ak} = \max_i(\sigma_{ik}), \qquad \boldsymbol{\sigma}_{Sk} = \max_i(\sigma_{ik}) \tag{18}$$

This method focuses on the overall importance of an actuator or sensor regardless of its importance to a specified mode, so it could possibly result in large indices from the higher modes. It does not agree with the design goal for base isolation systems where the first several modes dominate, so it is not adopted in this study.

One may also examine the importance of all control devices/sensors to a single mode, i.e., columns of the matrices (16), using row Eq. (19):

$$\text{Controller index vector:} \quad \boldsymbol{\sigma}_{Am} = [\boldsymbol{\sigma}_{Am1} \quad \boldsymbol{\sigma}_{Am2} \quad \cdots \quad \boldsymbol{\sigma}_{Amn}] \tag{19a}$$

$$\text{Sensor index vector:} \quad \boldsymbol{\sigma}_{Sm} = [\boldsymbol{\sigma}_{Sm1} \quad \boldsymbol{\sigma}_{Sm2} \quad \cdots \quad \boldsymbol{\sigma}_{Smn}] \tag{19b}$$

where

$$\boldsymbol{\sigma}_{Ami} = \sqrt{\sum_j^s \sigma_{ij}^2}, \qquad \boldsymbol{\sigma}_{Smi} = \sqrt{\sum_k^r \sigma_{ik}^2} \tag{20}$$

This method (Gawronski 1998) characterizes the contribution of each device to each mode. Locations with small indices for lower modes would be removed. This method is adopted to determine the index vector for every available device location.

4.3 Exclusion of high-correlated locations

When one considers the placement of a very large number of candidate locations, the maximum placement indices alone may not be a sufficient criterion. Suppose that a specific location gives a high-performance index.

$$\begin{bmatrix} \sigma_{11} & \sigma_{21} & \cdots & \sigma_{i1} & \cdots & \sigma_{n1} \\ \sigma_{21} & \sigma_{22} & \cdots & \sigma_{i2} & \cdots & \sigma_{n2} \\ \cdots & \cdots & \cdots & \cdots & \cdots & \cdots \\ \sigma_{1k} & \sigma_{2k} & \cdots & \sigma_{ik} & \cdots & \sigma_{nk} \\ \cdots & \cdots & \cdots & \cdots & \cdots & \cdots \\ \sigma_{1s} & \sigma_{2s} & \cdots & \sigma_{is} & \cdots & \sigma_{ns} \end{bmatrix} \Longleftarrow j\text{th mode} \tag{16}$$
$$\Uparrow$$
$$j\text{th mode}$$

Inevitably, locations close to it will have a high-performance index as well. But the locations in the neighborhood are not necessarily the best choice because the performance gains achieved using these devices can also be achieved by appropriate gain adjustments. The best strategy is to find locations that cannot be compensated for by gain adjustment. Here, correlation coefficients are introduced to remove highly correlated locations (Gawronski 1998).

Given a vector of the squares of the i^{th} Hankel modal norms, the correlation coefficient ρ_{ik} is defined as Eq. (21). Then, given a small positive number ε, say $\varepsilon = 0.001$, denote the membership index $I(k)$, $k = 1, \cdots, r$, where r is the number of sensors (control devices). The membership index is determined as Eq. (22).

$$\boldsymbol{g}_i = \begin{bmatrix} \|G_{i1}\|_h^2 \\ \|G_{i2}\|_h^2 \\ \vdots \\ \|G_{in}\|_h^2 \end{bmatrix} \qquad \rho_{ik} = \frac{\boldsymbol{g}_i^T \boldsymbol{g}_k}{\|\boldsymbol{g}_i\|_2 \|\boldsymbol{g}_k\|_2}, \tag{21}$$
$$k = i+1, \cdots, r, \qquad i = 1, \cdots, r.$$

$$I(k) = \begin{cases} 0, & \rho_{ik} > 1-\varepsilon \quad \text{and} \quad \sigma_k < \sigma_i \text{ for } k > i \\ 1, & \text{elsewhere} \end{cases}. \tag{22}$$

If $I(k) = 1$, then the k^{th} sensor (actuator) is accepted. If $I(k) = 0$, the k^{th} sensor (actuator) is rejected. In the case of $I(k) = 0$, the two locations i and k are either highly correlated ($\rho_{ik} > 1-\varepsilon$), or the i^{th} location has a higher performance $\boldsymbol{\sigma}_i$.

Based on the above analysis, the placement strategy is established.

4.4 Placement procedures

The benchmark problem requires that, the control force should not exceed the bearing forces, and not to exceed 10% of the total weight of the structural system for practicality. The total weight of the building is 2.031×10^5 kN. Simulations show that the maximum bearing forces for the passive isolation case are 33%, 18%, and 21% of the total weight in the x-, y-, and r-directions, respectively.

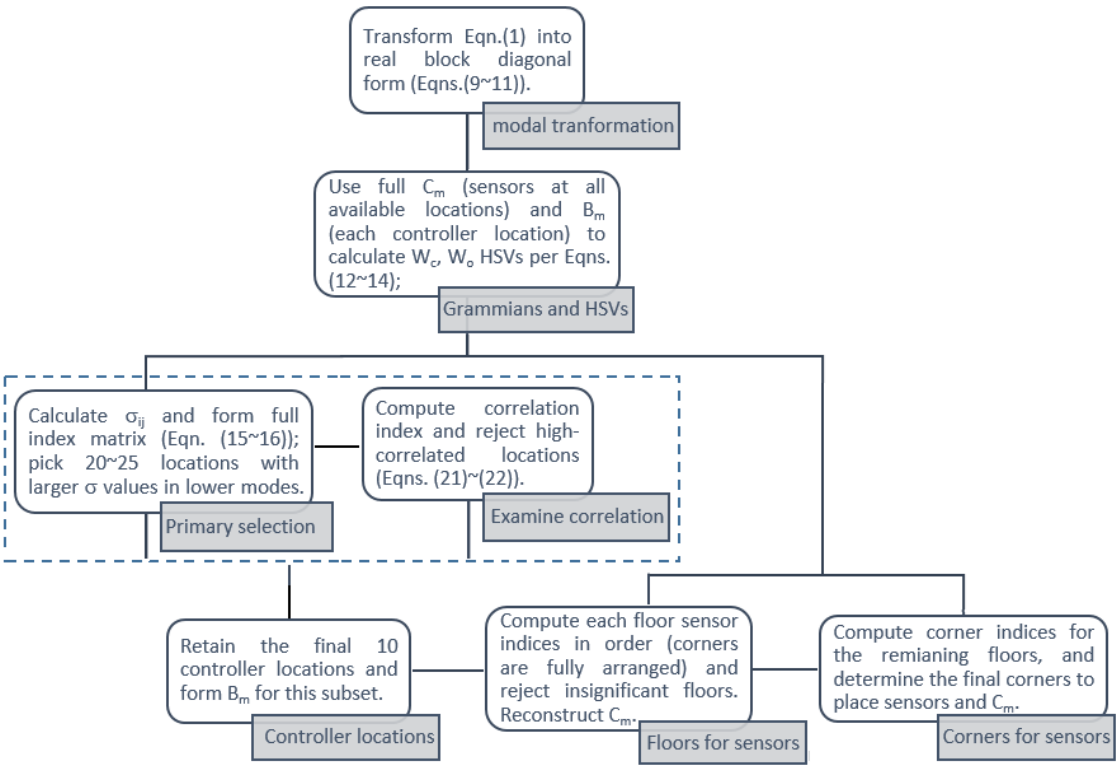

Fig. 3 Flowchart of the placement approach

Assume that the capacity of each control devices is 1000 kN, and each location put 2 controllers, the total number of locations in each direction should not exceed 10.

The placement procedure can be divided into three steps:

- Transfer the equation into real block modal form
- Determine the controller locations: form the 92×27 (total 27 modes) controller placement index matrix, and choose those with larger index and lower correlation.
- Determine the important floors for sensors. Then, for the remaining floors, determine the important corners.

The procedures are shown in the flowchart of Fig. 3.

5. Placement results

Control device (e.g., MR damper) locations are to be determined first. Assume accelerometers are placed at all story corners, one in *x*- and one in *y*- (namely, full sensor placement). Place control devices at bearing location #1, one in the *x*- and one in the *y*-. Follow the placement procedures, use Eqs. (13), (14) and (19) to compute placement indices of all modes. Repeat this process for all other 91 bearing locations. The resulting control device placement index matrix has a dimension of 92×27. Fig. 4 shows the indices of first 18 modes (first 6 modes in *x*-, *y*- and *r*-directions, respectively) versus bearing locations.

Fig. 4 shows that, where placement indices in the *x*-, *y*-directions are large, those in the *r*-direction are small. For the most interested isolation modes (1, 2, 3), the indices are in the same order. Comparing Figs. 2 and 3, it is found that locations with large indices are mostly on the outer base corners and the south edge. Particularly, locations near corner 2 (bearing 19) and 4 (bearing 80) and the south edge, the r-direction indices are the largest, which agrees with the fact that they are the farthest points away from the center of mass. Locations that have large *x*-direction (mode 1, blue line) Hankel norms are along or near the south edge too, (bearing 1-3, 31, 60-65, 90, etc.). These locations are near the *x*-axis (across the center of the mass). The index change with different locations on y-direction (mode 2, red line) is not apparent. The reason might lies in the structural irregularity: it is more eccentric in *x*- than in *y*-. As a result, the *y*- index change with location are less significant comparing with that of *x*-. Anyway, it is still preferable to include points near the y-axis and the other corner (corner 1), though they do not show high indices from placement result. Taking into account all possible high correlations and including some inner locations and inner corners as well, the primary selected location numbers are (22 in total):

1, 2, 3, 12, 13, 19, 30, 31, 40, 43, 49, 62, 63, 64, 73, 74, 75, 80, 81, 87, 91, 92

The benchmark constraints require that the control force not exceed the bearing force, and it is desirable not to exceed 10% of the total weight of the structural system. The total weight of the building is 2.031×10^5 kN. Simulations show that the maximum bearing forces of the passive system are 33%, 18%, and 21% of the total weight in the *x*-, *y*-, and *r*-directions, respectively. If MR dampers are

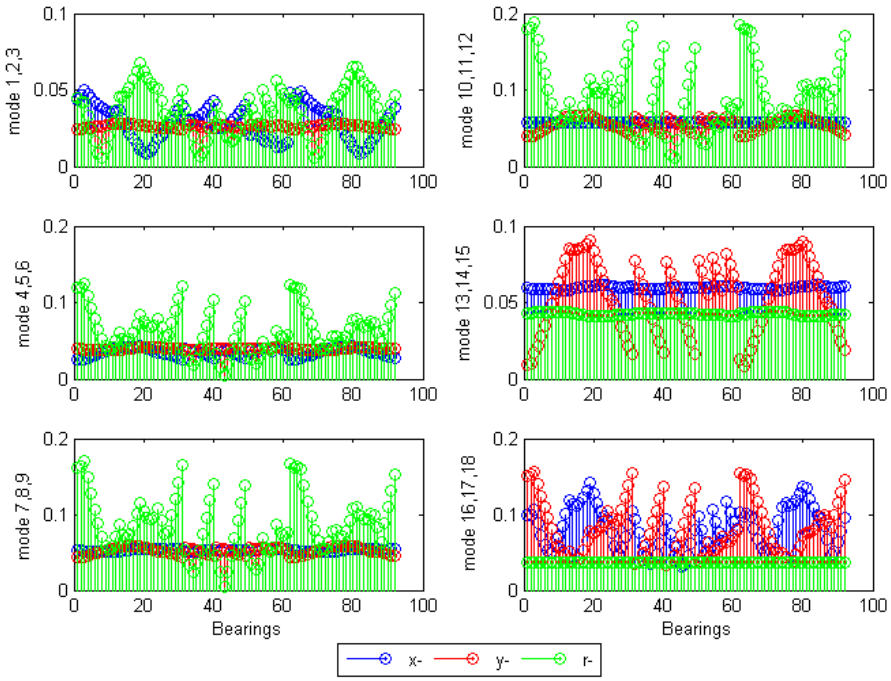

Fig. 4 Modal placement indices (18 modes) of bearing/controller of 92 locations

adopted as control devices, and assuming the capacity is 1000 kN each, the total number of MR dampers should not exceed 40. So, in this study, it was decided to use 40.

The next step is to reject the highly correlated locations. So first, set the small number $\varepsilon = 0.001$, i.e., locations i and k are regarded as highly correlated if $r_{ik} > 0.999$. Table 1 provides the membership indices (those with $I(k) = 0$ are

Table 1 Membership index of the control device locations

Location	1	2	3	12	13	19	30	31	40	43	49	62	63	64	73	74	75	80	81	87	91	92
1	0	1	1	1	1	1	1	1	1	1	1	1	1	1	1	1	1	1	1	1	1	0
2		0	1	1	1	1	1	1	1	1	1	1	0	0	1	1	1	1	1	1	1	0
3			0	1	1	1	1	0	1	1	1	0	0	0	1	1	1	1	1	1	1	1
12				0	1	1	1	1	1	1	1	1	1	1	1	1	1	1	1	1	1	1
13					0	1	1	1	1	1	1	1	1	1	1	1	1	1	1	1	1	1
19						0	1	1	1	1	1	1	1	1	1	1	1	0	0	1	1	1
30							0	1	0	1	0	1	1	1	1	1	1	1	1	1	0	1
31								0	1	1	1	1	0	0	1	1	1	1	1	1	1	0
40									0	1	0	1	1	1	1	1	1	1	1	1	0	1
43										0	1	1	1	1	1	1	1	1	1	1	1	1
49											0	1	1	1	1	1	1	1	1	1	0	1
62												0	0	0	1	1	1	1	1	1	1	0
63													0	1	1	1	1	1	1	1	1	0
64														0	1	1	1	1	1	1	1	0
73															0	1	1	1	1	1	1	1
74																0	1	1	1	1	1	1
75																	0	1	1	1	1	1
80																		0	0	1	1	1
81																			0	1	1	1
87																				0	1	1
91																					0	1
92																						0

Table 2 Correlated control device locations

Location	Correlated locations
1	92
2	92
3	31, 62, 63, 64
19	80, 81
30	40, 49
31	63, 64
40	49

to be rejected).

Based on Table 1, the original locations (1st column) and highly correlated locations (2nd column, $I(k) = 0$) are shown in Table 2. Location numbers that do not show up in this table, such as 12, 13, 72, 73, 74, have $I(k) = 1$ and thus are accepted.

Eliminating the highly correlated locations, there are 12 locations remaining. Considering planar distribution, 10 locations are finally selected. They are: 3, 13, 19, 30, 31, 43, 65, 74, 81, 87.

Next, sensor (accelerometer) floor placement indices are examined following placement procedures. Fig. 5 shows the first 18 mode indices versus floor numbers. Floor 0 represents the base.

Fig. 5 shows that, floors 0, 1 and 2 and the base always have small indices for modes 1-19, indicating that accelerometers placed on the base, 1st and 2nd floors do not give high observability, and thus are not very important in detecting acceleration signals. This result agrees with the engineering judgment for isolated buildings. So, accelerometers will be placed on floors 3 to 8.

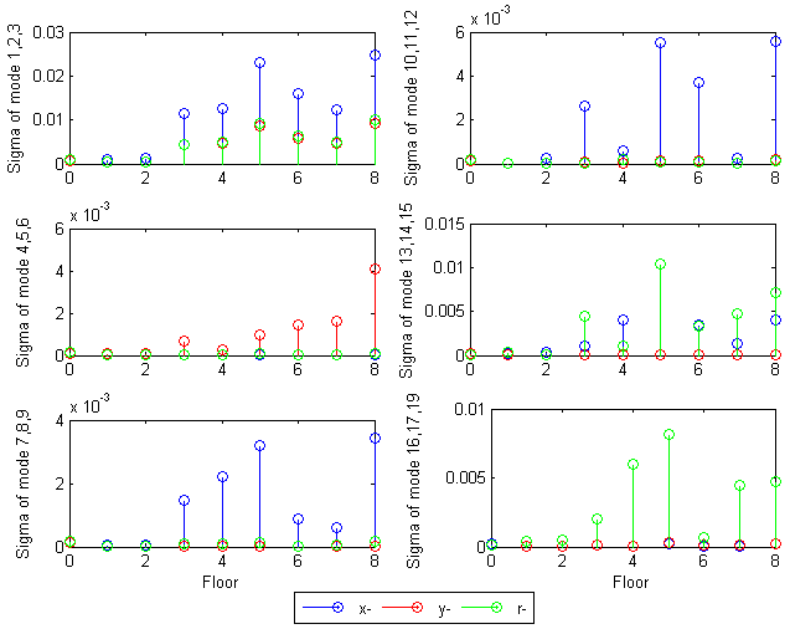

Fig. 5 Sensor placement indices of the first 18 modes of floors 0-8

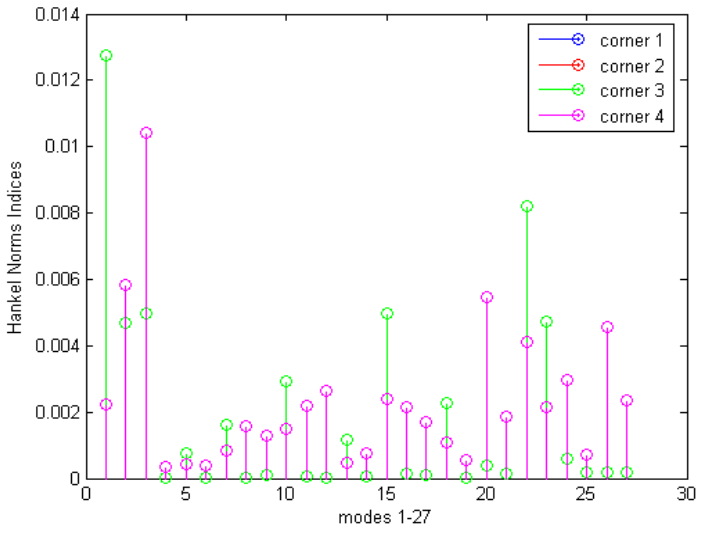

Fig. 6 Sensor corner placement indices for floor 3

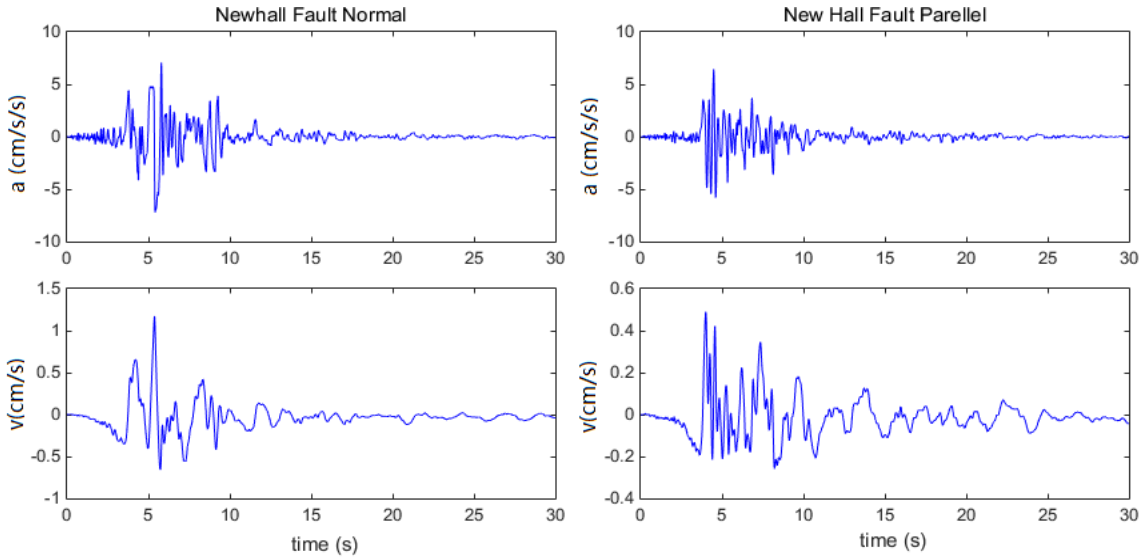

Fig. 7 Acceleration records and velocity time histories: the Newhall earthquake in two directions

Floors have four far-end corners, and thus eight available locations for accelerometers for each floor. Some of them are redundant. Three accelerometers per floor (24 total accelerometers) would provide a measure of all motions of that particular floor. So, the corner indices of floors 3 to 8 need to be computed. First, place two accelerometers (one in the *x*- and one in the *y*-) at each corner of floor 3; and then repeat the procedure for the remaining floors (4~8). Fig. 6 shows the sensor corner indices of floor 3.

Fig. 6 shows that, Hankel norm indices of corners 1, 2, and 3 (Fig. 2(b)) are identical, while those of corner 4 (magenta line) are different. Computation for floors 4~8 shows that, the indices corresponding to the four corners are the same. So not to loss generality, accelerometers are placed at corners 2 and 4 from floor 3 through 8. The two corners are the farthest points from the center of mass, and thus their responses are large. In addition, displacement sensors are placed at corners 2 and 4 at the isolation level to measure the bearing deformations. They are necessary for the determination of the control force. This completes the sensor placement. Note that the number of accelerometers could be further reduced if the indices were computed with accelerometers placed at single directions, because currently there are four accelerometers at each floor.

The locations of the accelerometers (red) and displacement sensors (yellow) are shown Fig. 2. It can be seen that no sensors are installed on floors 1 and 2.

To evaluate the effectiveness of the selected locations, time history analysis was performed using MR dampers as controllers and LQG method as control method. The LQG control objective is quadratic, with which Hankel norm on story responses agrees. So, the placement goal to achieve higher controllability and observability is expected to meet the control goal as well. This is the advantage of this placement strategy.

A typical near-fault earthquake, the Newhall earthquake, is selected as the excitation. Near-fault earthquakes contain rich frequency components and large low-frequency velocity impulses. Earthquakes with such characteristics are unfavorable to base isolation buildings, so are proper for this study. The Newhall earthquake is also one of the earthquakes stipulated by the benchmark problem to examine the control effects. The acceleration records and velocity and time histories (integrated from acceleration) of the Newhall earthquake in both fault normal and fault-parallel directions are shown in Fig. 7.

The optimum of the strategy-determined locations would be proved if its performance is better than other subsets. So, another set of locations (No. 42, 43, 44, 45, 51, 52, 53, 55, 56, 57, shown in Fig. 2) is selected for comparison, because the performance of this subset is apparently unreasonable: they are close to the center of mass of the floor (ineffective in controlling rotation) and are next to each other (highly correlated).

So three placement cases are compared: reduced sensor + optimal controller (blue lines), full sensor + optimal controller (red lines), and reduced sensor + unreasonable controllers (green lines). The time history responses of base drift, inter-story drift of the sixth floor, and roof acceleration of corner 1 in both *x*- and *y*- directions to the New Hall earthquake are shown in Fig. 8.

Comparing the responses with full sensor (red) and reduced sensor (blue) in Fig. 8, it shows that, in both *x*- and *y*- directions, the curves agree well, which means that, the reduced set of sensors is enough to capture the necessary structural response information for the controller. Also, comparing the responses of the strategy-determined subset devices (blue) and the unreasonable subset devices (green), it can be seen that, the strategy-determined subset leads to smaller responses than the unreasonable subset devices, no matter for base drift, inter-story drift of upper stories, and accelerations. The facts show that, the proposed Hankel-norm based strategy is effective in placing devices, i.e., it could achieve good control effects with smaller control effort.

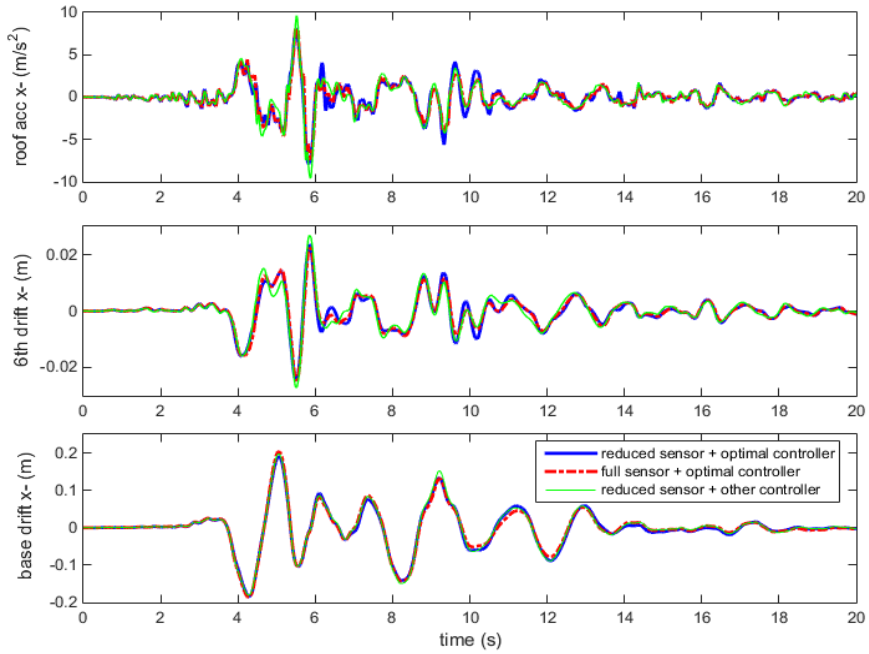

(a)

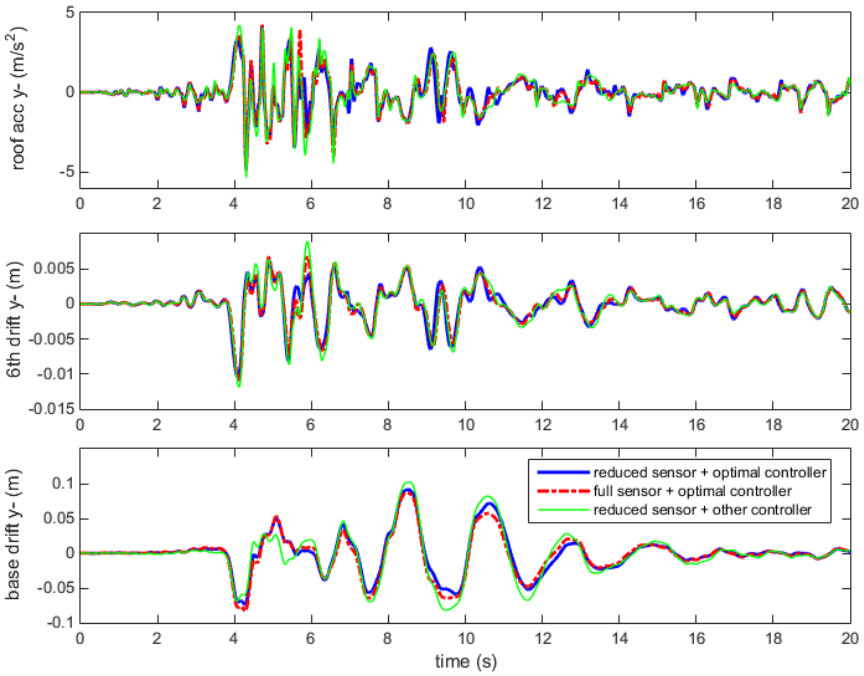

(b)

Fig. 8 Comparison of three device placements: (a) x- responses to the Newhall Earthquake; (b) y- responses to the Newhall Earthquake

6. Conclusions

A placement method based on modal Hankel norms were adopted in this paper to resolve the controller and sensor placement problem of a 3D irregular building, in which the candidate locations and number for controllers and sensors were restrained. The placement matrix was calculated in modal coordinates and normalized by modes to account for the influences of locations and modes. The final locations were determined by large index values and low correlations. With the method, ten "optimal" controller locations and eighteen sensor locations were determined. The efficiency of the method was confirmed by earthquake time history analyses, with MR dampers as controllers. Results showed that, the selected controller locations lead to better seismic control effects than other sets of controller locations, and the reduced sensors could capture enough information as full sensors did if the toleration is small enough. The results confirmed that, the modal Hankel norm-based index could efficiently determine the "optimal"

locations in the sense that the objective of "controllable and observable" is achieved. In the meantime, the method is explicit in physical concepts, easy to calculate by the approximate analytical equations in modal coordinates, and adaptable to LQG control strategies.

Acknowledgments

The research described in this paper was financially supported by the Mid-America Earthquake Center in part through NSF grant EEC-9701785, and its final completion and publication owed to the Natural Science Foundation of China #51578517.

References

Bigoni, C., Zhang, Z-Y. and Hesthaven, J.S. (2020), "Systematic sensor placement for structural anomaly detection in the absence of damaged states", *Comput. Methods Appl. Mech. Eng.*, **371**, 113315. https://doi.org/10.1016/j.cma.2020.113315

Bopardikar, S.D. (2021), "A randomized approach to sensor placement with observability assurance", *Automatica*, **123**, 109340. https://doi.org/10.1016/j.automatica.2020.109340

Boyd, S.P. and Barratt, C.H. (1991), *Linear Control Design*, Prentice Hall, Englewood Cliffs, NJ, USA.

Casciati, F. and Faravelli, L. (2014), "Sensor placement driven by a model order reduction (MOR) reasoning", *Smart Struct. Syst., Int. J.*, **13**(3), 343-352. https://doi.org/10.12989/sss.2014.13.3.343

Choi, J.W., Park, U.S. and Lee, S.B. (2000), "Measures of modal controllability and observability in balanced coordinates for optimal placement of sensors and actuators: a flexible structure application", *Proceedings of SPIE's 7th Annual International Symposium on Smart Structures and Materials*, Volume 3984, pp. 425-436, Newport Beach, CA, USA. https://doi.org/10.1117/12.388787

Gawronski, W.K. (1998), *Dynamics and Control of Structures*: *A Modal Approach*, Springer-Verlag Inc., New York, USA.

He, J., Xu, Y.L., Zhang, C.D. and Zhang, X.H. (2015), "Optimum control system for earthquake-excited building structures with minimal number of actuators and sensors", *Smart Struct. Syst., Int. J.*, **16**(6), 981-1002. https://doi.org/10.12989/sss.2015.16.6.981

Kang, S. and Shin, S. (2016), "Determination of optimal accelerometer locations for bridges using frequency-domain Hankel matrix", *J. Korea Inst. Struct. Maint. Inspection*, **20**(4), 27-34. https://doi.org/10.11112/jksmi.2016.20.4.027

Kaur, A., Kumar, P. and Gupta, G.P. (2019), "A weighted centroid localization algorithm for randomly deployed wireless sensor networks", *J. King Saud Univ. – Comput. Info. Sci.*, **31**(1), 82-91. https://doi.org/10.1016/j.jksuci.2017.01.007

Le, V., Li, X., Li, Y., Cao, Y. and Le, C. (2016), "Optimal placement of TCSC using controllability Gramian to damp power system oscillations", *Int. Transact. Electr. Energy Syst.*, **26**(7), 1493-1510. https://doi.org/10.1002/etep.2159

Leyder, C., Dertimanis, V., Frangi, A. and Lombaert, G. (2018), "Optimal sensor placement methods and metrics – comparison and implementation on a timber frame structure", *Struct. Infrastruct. Eng.*, **14**(7), 997-1010. https://doi.org/10.1080/15732479.2018.1438483

Lu, L., Wang, X., Liao, L., Wei, Y., Huang, C. and Liu, Y. (2015), "Application of model reduction technique and structural subsection technique on optimal sensor placement of truss structures", *Smart Struct. Syst., Int. J.*, **15**(2), 355-373. https://doi.org/10.12989/sss.2015.15.2.355

Majumder, S. and Khaparde, S.A. (2016), "Revenue and ancillary benefit maximization of multiple non-collocated wind power producers considering uncertainties", *IET Gener. Transm. Dis.*, **10**(3), 789-797.

Moore, B.C. (1981), "Principle component analysis in linear systems: controllability, observability, and model reduction", *IEEE Transact. Automatic Control*, **26**(1), 17-32. https://doi.org/10.1109/TAC.1981.1102568

Narasimhan, S., Nagarajaiah, S., Johnson, E.A. and Gavin, H.P. (2002), "Benchmark problem for control of base isolated buildings", *Proceedings of the 3rd World Conference on Structural Control*, Columbia University, New York, NY, USA, June.

Reichert, I., Olney, P. and Lahmer, T. (2020), "Combined approach for optimal sensor placement and experimental verification in the context of tower-like structures", *J. Civil Struct. Health Monitor.*, **11**(1), 223-234. https://doi.org/10.1007/s13349-020-00448-7

Silva, S.D., Lopes Jr., V. and Assunção, E. (2004), "Robust control to parametric uncertainties in smart structures using linear matrix inequalities", *J. Brazil Soc. Mech. Sci. Eng.*, **26**(4), 430-437.

Soman, R.N., Onoufrioua, T., Kyriakidesb, M.A., Votsisc, R.A. and Chrysostomou, C.Z. (2014), "Multi-type, multi-sensor placement optimization for structural health monitoring of long span bridges", *Smart Struct. Syst., Int. J.*, **14**(1), 55-70. https://doi.org/10.12989/sss.2014.14.1.055

Tong, K.H., Bakhary, N., Kueh, A.B.H. and Yassin, A.Y. (2014), "Optimal sensor placement for mode shapes using improved simulated annealing", *Smart Struct. Syst., Int. J.*, **13**(3), 389-406. https://doi.org/10.12989/sss.2014.13.3.389

Yang, S.M. (1997), "Stability analysis of linear structural control systems with noncolocated feedback", *Comput. Struct.*, **62**(4), 685-690. https://doi.org/10.1016/S0045-7949(96)00265-9

BS